DTU Library

High-power green light generation by second harmonic generation of single-frequency tapered diode lasers

Jensen, Ole Bjarlin; Andersen, Peter E.; Sumpf, Bernd; Hasler, Karl-Heinz; Erbert, Götz; Petersen, Paul Michael

Published in:
Proceedings of SPIE

Link to article, DOI:
10.1117/12.840879

Publication date:
2010

Document Version
Peer reviewed version

High power green light generation by second harmonic generation of single-frequency tapered diode lasers

Ole Bjarlin Jensen[*a], Peter E. Andersen[a], Bernd Sumpf[b], Karl-Heinz Hasler[b], Götz Erbert[b], and Paul Michael Petersen[a]

[a] DTU Fotonik, Department of Photonics Engineering, Frederiksborgvej 399, Dk-4000 Roskilde, Denmark.

[b]Ferdinand-Braun-Institut, Leibniz-Institut für Höchstfrequenztechnik, Optoelectronics Department, Gustav-Kirchhoff-Strasse 4, 12489 Berlin, Germany.

ABSTRACT

We demonstrate the generation of high power (>1.5W) and single-frequency green light by single-pass second harmonic generation of a high power tapered diode laser. The tapered diode laser consists of a DBR grating for wavelength selectivity, a ridge section and a tapered section. The DBR tapered laser emits in excess of 9 W single-frequency output power with a good beam quality. The output from the tapered diode laser is frequency doubled using periodically poled $MgO{:}LiNbO_3$. We investigate the modulation potential of the green light and improve the modulation depth from 1:4 to 1:50.

Keywords: Frequency doubling, second harmonic generation, SHG, tapered diode laser.

1. INTRODUCTION

Many applications within biomedicine, material processing and displays require light sources in the visible region. Display applications in particular require compact and efficient red, green and blue light sources with good beam quality. The red and blue spectral regions are covered by direct emission from diode lasers based on GaAs and GaN, respectively. Diode laser emission in the green spectral region has recently been demonstrated with a few tens of milliwatts emitted in the range 515 nm to 531 nm [1,2]. High power emission from direct diode lasers are not expected in the near future and currently other methods are used to cover the green spectral region. For use in display applications, requirements are strict on power consumption, beam quality and physical size.

Several methods exist for efficient generation of green light. Frequency doubling of solid state or fiber lasers is the most well established method for green light generation. Many Watts can be generated with good spatial and spectral quality [3,4]. Green lasers based on solid state lasers have the disadvantage that the output cannot be easily modulated with high speeds because of the long carrier lifetime in the laser materials. High speed modulation is a requirement if the laser is to be used for display applications employing the flying-spot technique. The output from solid state lasers can be modulated externally for instance by use of acousto-optic modulators. However, this increases the complexity, size and cost of the laser system. Recently frequency doubled optically pumped semiconductor lasers have shown promising results obtaining high output powers in the visible spectral region [5,6]. The output from these lasers possesses high spatial and spectral quality and as they are based on semiconductor material the possibility of direct modulation of the output exists.

Direct frequency doubling of the output from diode lasers has been investigated extensively in recent years. Low power green light can be obtained by frequency doubling the output from single-mode DFB or DBR diode lasers in nonlinear waveguides [7]. The waveguides have very high conversion efficiency because of the tight confinement of the light in the waveguide. The tight confinement, however, also put an upper limit on the generated power from the waveguide in order to prevent damage to the waveguide [8]. Recently, a planar waveguide was used to increase the power handling abilities. 1.08 W of green light was obtained using a fiber laser as pump source [9] and 346 mW of green light was obtained using a master-oscillator power-amplifier (MOPA) [10]. The limited coupling efficiency of 20 % of the

[*] ojen@fotonik.dtu.dk; phone: +45 46774553; fax: +45 46774588; www.fotonik.dtu.dk

astigmatic and elliptical beam from the MOPA limited the output power. 600 mW of blue light at 488 nm was generated by frequency doubling the output from a MOPA in a bulk PPLN crystal [11].
The size and complexity of MOPA configurations limit their practical usability. High power tapered diode lasers with good spectral and spatial quality has become available resulting in a significant reduction of size and complexity compared to MOPA configurations. The spectral selectivity can be done using external cavity approaches [12] or using DFB or DBR gratings within the laser structure [13]. Recently more than 1 W of blue light and more than 1.5 W of green light were generated by single pass frequency doubling of DBR tapered lasers in bulk periodically poled crystals [14,15].
Here we present the generation of more than 1.5 W of green output power using a novel DBR tapered diode laser as pump source for the frequency doubling. More than 9 W of output power in a narrow line width nearly diffraction limited beam was generated by the DBR tapered laser. Frequency doubling was performed in a bulk periodically poled $MgO:LiNbO_3$ (PPMgLN) crystal. The green output has been modulated at 100 MHz by modulating the current to the ridge section of the laser. The modulation depth has been improved from 1:4 to more than 1:50 by detuning the DBR reflection from the gain maximum.

2. DBR TAPERED LASER

The tapered lasers used in this work are constructed as two-section devices with a 6[th] order surface grating embedded in the ridge section of the laser. A sketch of the DBR tapered laser is given in figure 1. The total laser cavity length is 6 mm. The 5 µm wide ridge waveguide section of the laser is 2 mm long and the taper section is 4 mm long with a 6º taper angle. The two sections are separately contacted to enable a direct modulation of the output by modulating only the current to the ridge waveguide section. The InGaAs triple quantum well is embedded in a 4.8 µm super large optical cavity (SLOC) providing a narrow vertical divergence of 15º (FWHM). The passive DBR mirror with a length of 1 mm is located at the rear end of the ridge waveguide section. A reflectivity of about 60 % of the DBR mirror was obtained. The laser is mounted p-side up on a CuW heat spreader mounted on a standard 25 mm x 25 mm copper heat sink for efficient heat removal from the laser.

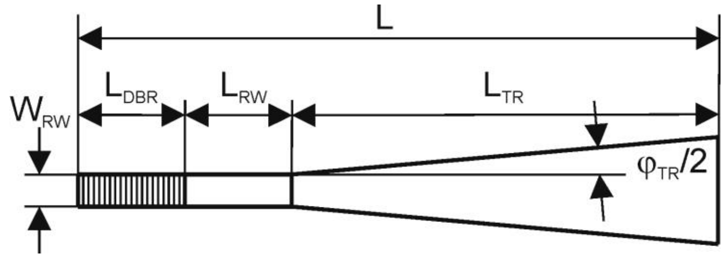

Fig. 1. Experimental setup of the external cavity tapered laser using a diffraction grating external cavity.

Current is supplied to the laser from two separate power supplies. One power supply is used for the ridge waveguide section and delivers a maximum of 300 mA. The tapered section is supplied with a current of up to 14 A. The two sections of the laser have common ground. The laser is capable of delivering more than 9 W of output power when 300 mA and 14 A are supplied to the ridge and taper sections, respectively. The power current characteristics at 15ºC operating temperature are shown in figure 2. The laser threshold is approximately 2.1 A and the slope efficiency of the laser is approximately 0.8 W/A when changing the taper current. Up to the maximum obtained output power, the laser power shows no sign of roll-over. The beam quality of the laser at 14 A taper section current was measured as M^2 ($1/e^2$) < 1.3 for both the fast and slow axis of the laser. Approximately 70 % of the laser power was contained in the central lobe of the beam in the slow axis direction. Results on similar DBR tapered lasers have previously shown up to 12 W output power in a near diffraction limited beam [16].

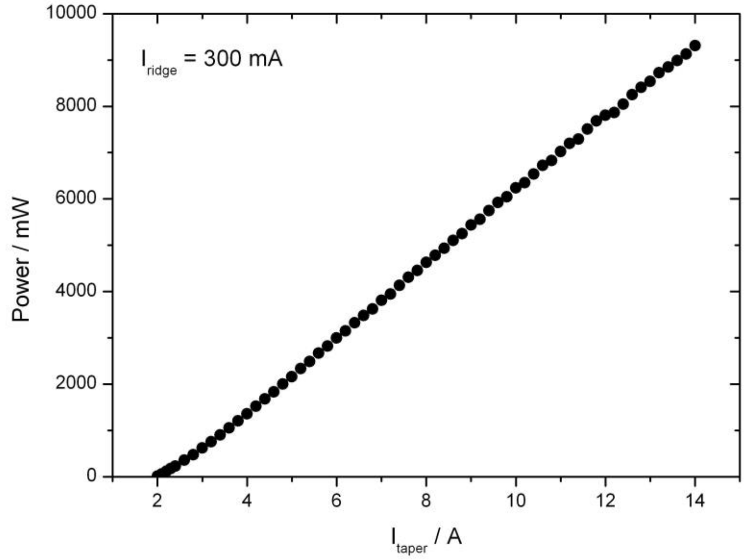

Fig. 2. Power current characteristics for the DBR tapered laser at a ridge section current of 300 mA and an operating temperature of 15ºC.

The laser wavelength is determined by the DBR grating. The output spectrum at14.3ºC operating temperature and 14 A taper current is given in figure 3. This temperature is used as the obtained wavelength facilitated phase match in the frequency doubling experiments. The laser line width is limited by the resolution of the optical spectrum analyzer (Advantest Q8347) to 6 pm. The side mode suppression is larger than 25 dB limited by the dynamic range of the spectrum analyzer.

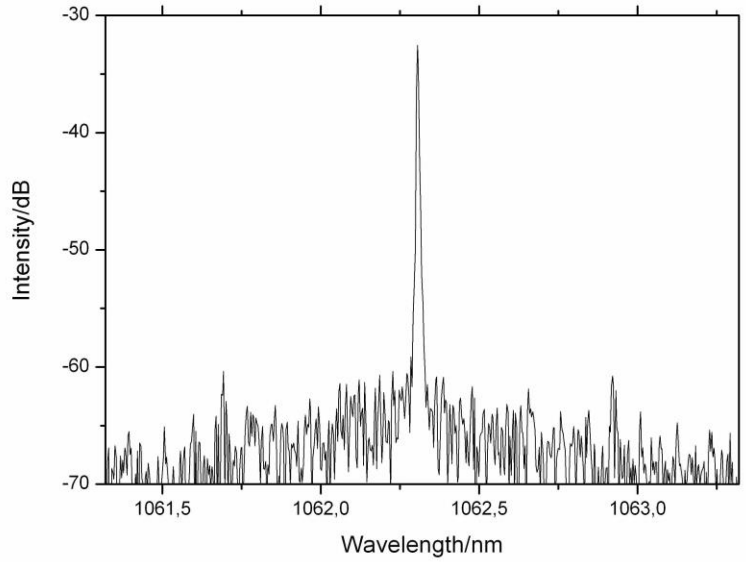

Fig. 3. Spectrum of the DBR tapered laser at 14.3ºC operating temperature and 14 A taper current.

The laser wavelength is dependent on the current to the ridge section, the current to the taper section and the laser temperature. The wavelength dependency on the taper current and the operating temperature was investigated and the results are given in figure 4. Above 6 A taper section current, the wavelength follows a linear trend when the taper current is increased. The wavelength change is approximately 23 pm/A. The curve shows the typical variations well known from DBR lasers. The wavelength dependency on the laser temperature is approximately linear with a slope of 87 pm/K. Changing the temperature leads to occasional mode hops and one mode hop is evident in figure 4.

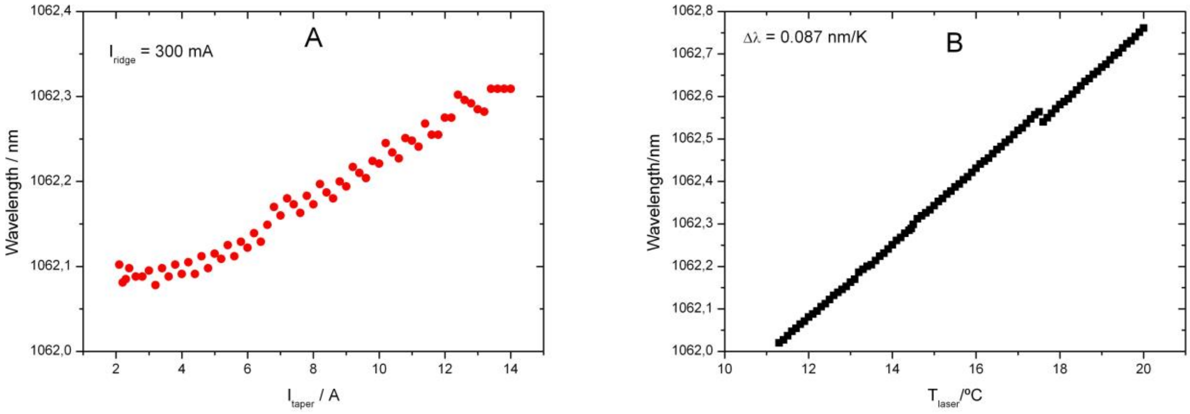

Fig. 4. Wavelength vs. taper section current at fixed ridge current of 300 mA and 15ºC operating temperature (A). Wavelength vs. operating temperature at 300 mA ridge section current and 14 A taper section current (B).

The laser power can be modulated by modulating the ridge section current. As the ridge section is applied with currents below 300 mA it is considerably easier to modulate this current at high speeds than the taper section current of more than 10 A. We have modulated the current to the ridge section with 50 % duty cycle and approximately 100 mA current at 100 MHz modulation speed. At room temperature, the modulation depth is approximately 1:2 as seen in figure 5.

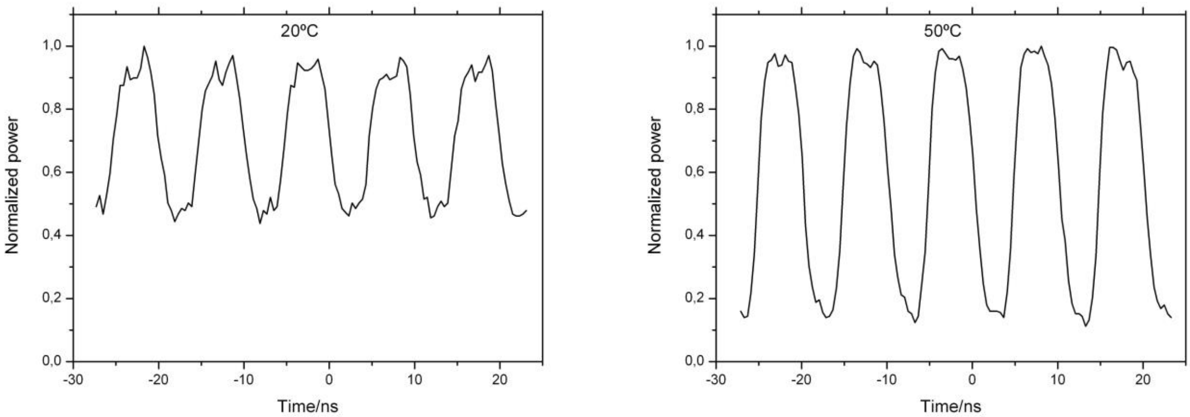

Fig. 5. Modulated output from the laser at 20ºC operating temperature (left) and at 50ºC operating temperature (right).

This modulation depth is relatively low and will only lead to a small modulation depth of the generated green light. This low modulation depth is caused by the good match between the DBR grating reflectivity and the gain maximum of the laser material. The laser is emitting laser light even though no current is flowing through the ridge section of the laser. If the DBR grating reflectivity and the laser gain curve are detuned, it is possible to stop the laser action at zero ridge section current. A detuning can be obtained by changing the laser temperature as the DBR grating reflectivity will be tuned less than the gain maximum. We have investigated the possibility of improving the modulation depth by increasing the laser temperature and thus shifting the gain curve away from the DBR grating reflectivity. By increasing the temperature of the laser to 50ºC the modulation depth is improved to approximately 1:6 as evident from figure 5. Increasing the laser temperature to 50ºC decreases the output power significantly to approximately 5 W in CW operation. The spectrum is shifted due to the increased temperature but the spectral width is still limited by the resolution of the optical spectrum analyzer. The spatial properties of the laser are almost unchanged. By designing a detuning of the DBR reflectivity and gain curve of the laser it will be possible in future lasers to achieve good modulation capabilities at room temperatures and thus operate with high output power.

3. SECOND HARMONIC GENERATION

The DBR tapered laser was used as a pump source for second harmonic generation. The setup for the experimental investigations is sketched in figure 6.

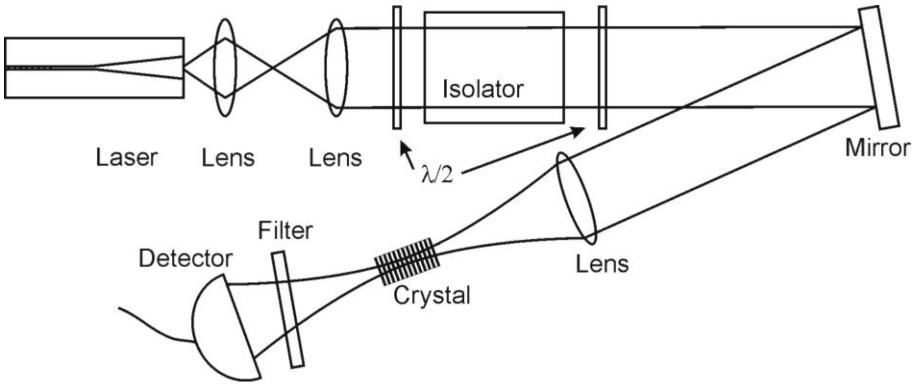

Fig. 6. Sketch of the experimental setup used for frequency doubling of the DBR tapered laser.

The DBR tapered laser is mounted on a temperature controlled base plate. The output from the laser is astigmatic and thus two lenses are required to collimate the beam and correct for astigmatism. We use a 3.1 mm focal length aspherical lens to collimate the beam in the fast axis and a cylindrical lens with 15 mm focal length to collimate the slow axis, correct for astigmatism and obtain an approximately symmetrical output beam in the two axes. The beam is send through a combination of two half wave plates and an optical isolator. This arrangement allows for adjustment of the power level while operating the laser under constant conditions. This is necessary as the collimating lenses are aligned for a fixed amount of astigmatism and the astigmatism will change when the operating conditions change. Rotation of the first half wave plate in combination with the polarizing beam splitter in the optical isolator will decrease the power after the isolator. The second half wave plate is used to correct the polarization after the optical isolator. A folding mirror and a focusing lens with 100 mm focal length are used to direct and focus the beam in the nonlinear crystal. The beam waist radius in the crystal is approximately 60 µm. This is significantly larger than the optimum beam waist of 29 µm predicted by the theory of Boyd and Kleinman [17] but proved to give the best conversion efficiency. This discrepancy may be explained by the non-Gaussian beam profile of the tapered laser. A dichroic filter is inserted in the output beam to avoid the residual light at 1062 nm.

The nonlinear crystal is a periodically poled MgO:$LiNbO_3$ (PPMgLN) crystal supplied by HCPhotonics. The crystal is 0.5 x 2 x 30 mm^3 (height x width x length) and the end facets are cut with an angle of 10º in the width direction and anti-reflection coated at 1064 nm and 532 nm to avoid back reflections to the laser. The poling period of the crystal is 6.92 µm. The crystal is kept in a temperature controlled oven to enable phase matching. In the CW experiments, the temperature was kept at 35ºC.

The laser temperature was set to 14.3ºC as this provided a laser wavelength of 1062.3 nm which gave optimum phase matching in the PPMgLN crystal. After passing the optical isolator and the optical components, 8.52 W is available before the PPMgLN crystal. 1.58 W of green output power at a wavelength of 531.15 nm was obtained after the dichroic filter. The second harmonic output power characteristics are shown in figure 7. Using the undepleted pump approximation, a quadratic relationship between the generated second harmonic power and the input fundamental power exist given by

$$P_{SHG} = \eta_{SHG} P_{laser}{}^{2} \tag{1}$$

Here P_{laser} and P_{SHG} are the power at the fundamental and second harmonic wavelength, respectively, while η_{SHG} is the nonlinear conversion efficiency. When the power conversion becomes sufficiently high, the undepleted pump approximation fails to reconstruct the experimental results and a more accurate expression is needed. The theoretical expression for the second harmonic power vs. the input fundamental power is given by

$$P_{SHG} = P_{laser} \tanh^2(\sqrt{\eta_{SHG} P_{laser}}) \tag{2}$$

In figure 7, the theoretical curves have been included for comparison using a nonlinear conversion efficiency η_{SHG} = 2.5 %/W. At an input power level below approximately 3.5 W, both curves follow the experimental results while at higher power levels, the depleted pump approximation provides the most accurate fit. The power conversion efficiency in the experiments is 18.5 % and the wall-plug efficiency is approximately 5 %. The generated second harmonic beam is nearly diffraction limited with $M^2 < 1.3$ ($1/e^2$).

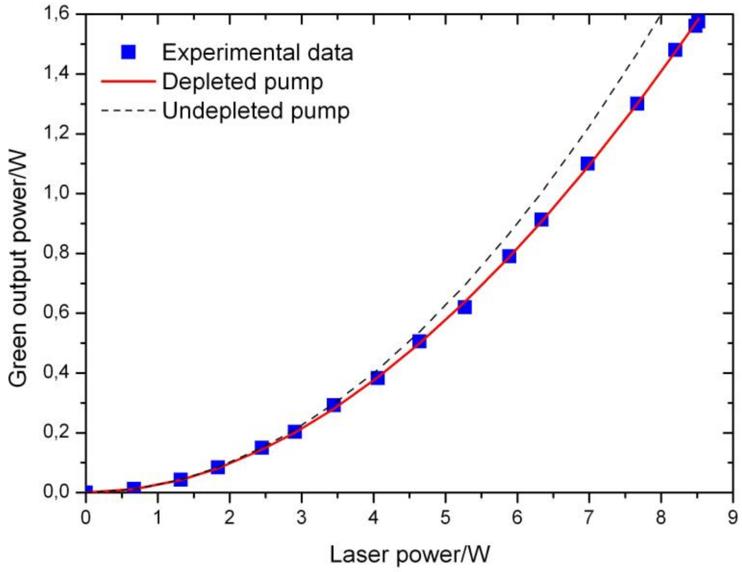

Fig. 7. Second harmonic output power vs. input fundamental power. A numerical fit using the depleted pump approximation (solid red line) and the undepleted pump approximation (dashed black line) using η_{SHG} = 2.5 %/W is included.

The power of the generated second harmonic output beam is sensitive to changes in the laser wavelength and the temperature of the PPMgLN crystal. A change leads to a phase mismatch that results in lower conversion efficiency. The laser wavelength can be tuned by changing the laser temperature as shown in figure 4 (B) and the PPMgLN temperature can be easily changed by adjusting the set point temperature of the crystal oven. The acceptance bandwidths of the PPMgLN crystal can be calculated using [18]

$$\Delta\lambda_{FWHM} = \frac{0.4429\,\lambda}{L}\left|\frac{n_2 - n_1}{\lambda} + \frac{\partial n_1}{\partial\lambda} - \frac{\partial n_2}{2\partial\lambda}\right|^{-1} \tag{3}$$

for the wavelength acceptance bandwidth and

$$\Delta T_{FWHM} = \frac{0.4429\,\lambda}{L}\left|\frac{\partial\Delta n}{\partial T} - \alpha\Delta n\right|^{-1} \tag{4}$$

for the temperature acceptance bandwidth respectively. In equation (3) and (4), λ is the laser wavelength, L is the crystal length, n is the refractive index and α is the coefficient of linear thermal expansion. Using the Sellmeier equations, its derivatives and the thermal expansion coefficient for $MgO{:}LiNbO_3$ it is possible to calculate the expected acceptance bandwidths for the nonlinear interaction. In figure 8, the measured wavelength and temperature tuning curves are shown for an input laser power of 1 W and 8.5 W. The theoretically calculated curves are included for comparison. As evident from the figure, the acceptance curves are broadening at higher input power. This is believed to be caused by heating of the PPMgLN crystal due to absorption. Furthermore, the phase matching temperature is slightly shifted at high input power confirming that the actual crystal temperature is increased by the absorption.

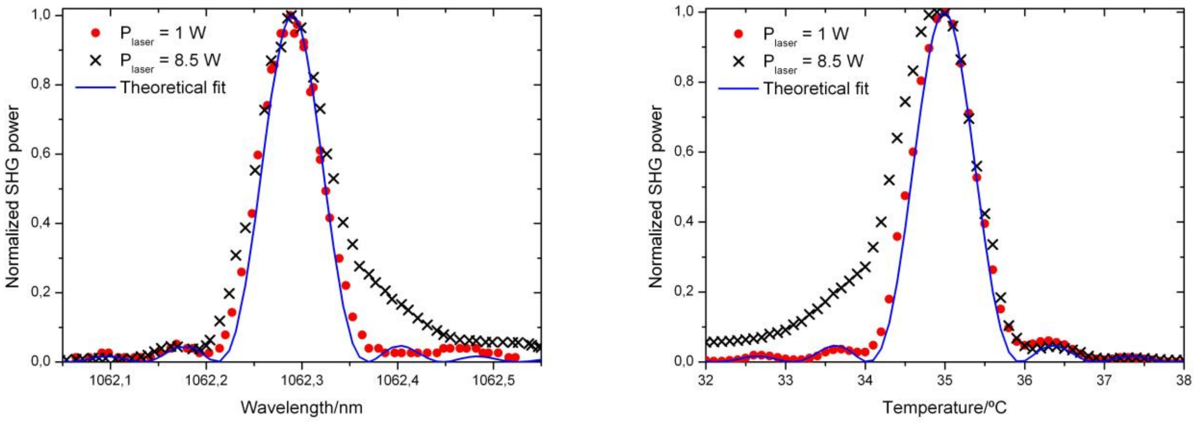

Fig. 8. Wavelength tuning curve (left) and PPMgLN temperature tuning curve at 1 W input laser power (red dots) and 8.5 W input power (black crosses). A theoretical fit based on equation (3) and (4) is included (blue line).

The modulation behavior of the second harmonic follows the modulation behavior of the fundamental beam. The nonlinear dependency of the second harmonic power on the input fundamental power will lead to an increased modulation depth in the second harmonic beam. It is expected that the modulation depth follows an approximately quadratic dependency of the fundamental modulation depth according to equation (1) and (2). A further increase in modulation depth can be expected as it has previously been shown that the laser wavelength and the astigmatism is slightly affected by the actual ridge section current applied [16]. The modulation behavior of the second harmonic output beam is shown in figure 9 for two different laser temperatures. The PPMgLN temperature has been increased to ensure phase matching at the changed laser wavelength. At 20ºC the modulation depth is approximately 1:4 in good agreement with the modulation depth of 1:2 in the fundamental beam. Increasing the laser temperature to 50ºC increases the laser modulation depth to 1:6 and the modulation depth in the second harmonic beam is higher than 1:50. The larger than quadratic increase in modulation depth at 50ºC operating temperature indicates that the wavelength shift and change in astigmatism has increased the modulation depth. At 50ºC operating temperature and 0 mA ridge section current, the laser is below threshold and thus only emitting spontaneous emission. The spectral bandwidth of the spontaneously emitted light is larger than the acceptance bandwidth of the PPMgLN crystal and this will also increase the modulation depth.

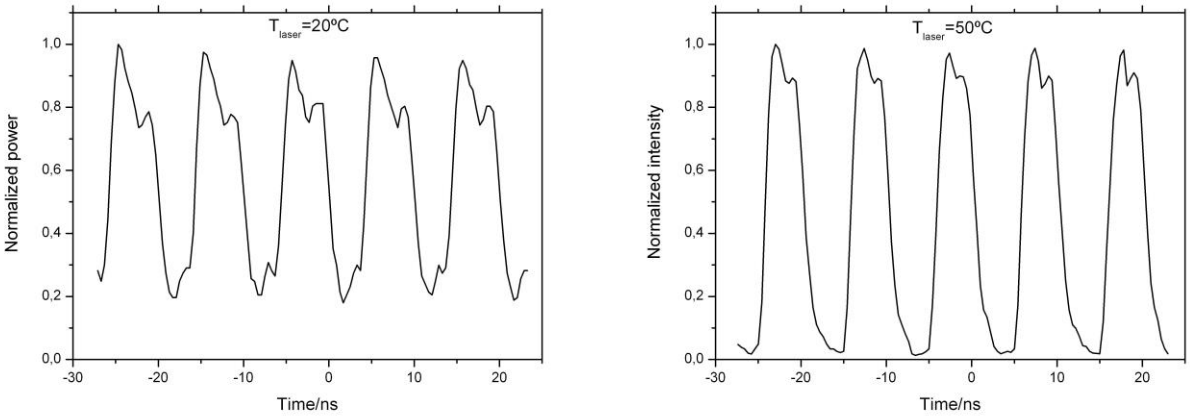

Fig. 9. Modulated green output at laser temperatures of 20ºC (left) and 50ºC (right), respectively.

4. CONCLUSION

Generation of 1.58 W of green light has been demonstrated employing a DBR tapered laser in single-pass second harmonic generation in a PPMgLN crystal. The DBR tapered diode laser emits more than 9 W of nearly diffraction limited output power with a narrow spectral bandwidth. The modulation behavior of the DBR tapered diode laser has been investigated and the modulation depth has been optimized by detuning the gain curve from the DBR reflectivity curve. This has resulted in an increased modulation depth for the second harmonic beam from 1:4 at room temperature to more than 1:50 at 50ºC operating temperature.

ACKNOWLEDGEMENT

The project was supported by the European Community in the project WWW.BRIGHTER.EU (IP 035266). The authors acknowledge the technical support of P. Jensen and H. E. Larsen.

REFERENCES

[1] Miyoshi, T., Masui, S., Okada, T., Yanamoto, T., Kozaki, T., Nagahama, S. and Mukai, T., "510-515 nm InGaN-based green laser diodes on c-plane GaN substrate" Appl. Phys. Express 2, 062201 (2009).

[2] Enya, Y., Yoshizumi, Y., Kyono, T., Akita, K., Ueno, M., Adachi, M., Sumitomo, T., Tokuyama, S., Ikegami, T., Katayama, K. and Nakamura T., "531 nm green lasing of InGaN based laser diodes on semi-polar {2021} free-standing GaN substrates", Appl. Phys. Express 2, 082101 (2009).

[3] McDonagh, L. and Wallenstein, R., "Low-noise 62 W CW intracavity-doubled TEM_{00} $Nd:YVO_4$ green laser pumped at 888 nm," Opt. Lett. 32, 802-804 (2007).

[4] Tovstong, S. V., Kurimura, S. and Kitamura, K., "High power continuous-wave green light generation by quasiphase matching in Mg stoichiometric lithium tantalate," Appl. Phys. Lett. 90, 051115 (2007).

[5] Lee, J., Lee, S., Kim, T. and Park, Y., "7 W high-efficiency continuous-wave green light generation by intracavity frequency doubling of an end-pumped vertical external-cavity surface emitting semiconductor laser", Appl. Phys. Lett. 89, 241107 (2006).

[6] Fallahi, M., Fan, L., Kaneda, Y., Hessenius, C., Hader, J., Li, H., Moloney, J. V., Kunert, B., Stolz, W., Koch, S. W., Murray, J. and Bedford, R., "5-W yellow laser by intracavity frequency doubling of high-power vertical-external-cavity surface-emitting laser", IEEE Photon. Technol. Lett. 20, 1700-1702 (2008).

[7] Nguyen, H. K., Hu, M. H., Nishiyama, N., Visovsky, N. J., Li, Y., Song, K., Liu, X., Gollier, J., Hughes, L. C., Bhat, R. and Zah, C.-E., "107-mW low-noise green-light emission by frequency doubling of a reliable 1060 nm DFB semiconductor laser diode," IEEE Photon. Technol. Lett. 18, 682-684 (2006).

[8] Iwai, M., Yoshino, T., Yamaguchi, S., Imaeda, M., Pavel, N., Shoji, I. and Taira, T., “High-power blue generation from a periodically poled MgO:$LiNbO_3$ ridge-type waveguide by frequency doubling of a diode end-pumped Nd:$Y_3Al_5O_{12}$ laser,” Appl. Phys. Lett. 83, 3659-3661 (2003).

[9] Sakai, K., Koyata, Y. and Hirano, Y. “Planar-waveguide quasi-phase-matched second-harmonic-generation device in Y-cut MgO-doped $LiNbO_3$,” Opt. Lett. 31, 3134-3136 (2006).

[10] Sakai, K., Koyata, Y., Shimada, N., Shibata, K., Hanamaki, Y., Itakura, S., Yagi, T. and Hirano, Y., “Master-oscillator power-amplifier scheme for efficient green-light generation in a planar MgO:PPLN waveguide,” Opt. Lett. 33, 431-433 (2008).

[11] Maiwald, M., Schwertfeger, S., Güther, R., Sumpf, B., Paschke, K., Dzionk, C., Erbert, G. and Tränkle, G., “600 mW optical output power at 488 nm by use of a high-power hybrid laser diode system and a periodically poled MgO:$LiNbO_3$ bulk crystal,” Opt. Lett. 31, 802-804 (2006).

[12] Chi, M., Jensen, O. B., Holm, J., Pedersen, C., Andersen, P. E., Erbert, G., Sumpf, B. and Petersen, P. M., "Tunable high-power narrow-linewidth semiconductor laser based on an external-cavity tapered amplifier," Opt. Express 13, 10589-10596 (2005).

[13] Parke, R., Welch, D. F., Hardy, A., Lang, R., Mehuys, D., O’Brien, S., Dzurko, K. and Scifres, D., “2.0 W CW, diffraction-limited operation of a monolithically integrated master oscillator power amplifier,” IEEE Photon. Technol. Lett. 5, 297-300 (1993).

[14] Fiebig, C., Sahm, A., Uebernickel, M., Blume, G., Eppich, B., Paschke, K. and Erbert, G., “Compact second-harmonic generation laser module with 1 W optical output power at 490 nm“, Opt. Express 17, 22785-22790 (2009).

[15] Jensen, O. B., Andersen, P. E., Sumpf, B., Hasler, K.-H., Erbert, G. and Petersen, P. M., “1.5 W green light generation by single-pass second harmonic generation of a single-frequency tapered diode laser”, Opt. Express, 17, 6532-6539 (2009).

[16] Sumpf, B., Hasler, K.-H., Adamiec, P., Bugge, F., Fricke, J., Ressel, P., Wenzel, H., Erbert, G. and Tränkle, G., “1060 nm DBR tapered laser with 12 W output power and a nearly diffraction limited beam quality“, Proc. SPIE, 7230, 72301E-1 (2009).

[17] Boyd, G. D. and Kleinman, D. A., “Parametric Interaction of Focused Gaussian Light Beams,” J. Appl. Phys. 39, 3597-3639 (1968).

[18] Fejer, M. M., Magel, G. A., Jundt, D. H. and Byer, R. L.,” Quasi-Phase-Matched Second Harmonic Generation: Tuning and Tolerances,” IEEE J. Quantum Electron. 28, 2631-2654 (1992).